Structural Eng./Earthquake Eng., JSCE, Vol. 17, No. 2, 149s-162s, 2000 July
(J. Struct. Mech. Earthquake Eng., JSCE, No. 654/ I-52)

INELASTIC SEISMIC RESPONSE ANALYSIS OF ECCENTRICALLY LOADED STEEL BRIDGE PIERS

Qingyun LIU[1], Tsutomu USAMI[2] and Akira KASAI[3]

[1] Student Member of JSCE, M. of Eng., Graduate Student, Dept. of Civil Eng., Nagoya University
(Furocho, Chikusa-ku, Nagoya 464-8603, Japan)
[2]Fellow of JSCE, Dr. of Eng., Dr. of Sc., Professor, Dept. of Civil Eng., Nagoya University
(Furocho, Chikusa-ku, Nagoya 464-8603, Japan)
[3]Member of JSCE, M. of Eng., Research Associate, Dept. of Civil Eng., Nagoya University
(Furocho, Chikusa-ku, Nagoya 464-8603, Japan)

This paper presents a simple SDOF formulation for inelastic seismic response analysis of eccentrically loaded steel bridge piers, considering the vertical inertia associated with horizontal ground motion. Modeling of the unsymmetrical hysteretic behavior is verified by pseudodynamic test results. It is shown that influence of vertical inertia force can not be neglected when e/h (e = eccentricity, h = pier height) is relatively large. A parametric study shows that under Level 2 accelerograms, steel bridge piers with intermediate eccentricity (e/h around 0.1～0.2) are susceptible to highest maximum displacement; And eccentricity definitely leads to higher residual displacement level than centrally loaded steel bridge piers.

Key Words: *eccentrically loaded, steel bridge piers, seismic analysis, inelastic behavior*

1. INTRODUCTION

Due to different ground area conditions, highway bridge piers take different shapes, and the load from some upper structures may act eccentrically on the supporting bridge piers. A survey of the existing steel bridge piers constructed by Nagoya Public Highway Corporation shows that maximum eccentricity rate, e/h (e = eccentric distance, h = height of the steel bridge pier), can be as large as 0.5. And a typical eccentrically loaded type is the inverted L-shaped steel bridge piers (**Fig.1**).

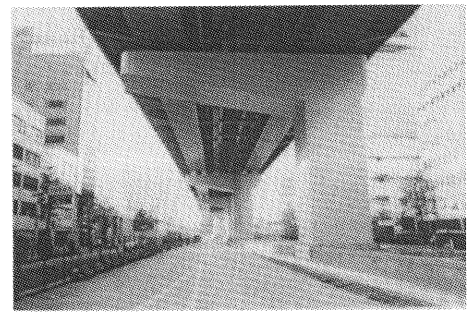

Fig.1 Inverted L-shaped steel bridge pier (Nagoya Expressway)

So far, extensive experimental and analytical researches have been done on seismic performance of centrally loaded T-shaped steel bridge piers, but there seems to be little corresponding information about eccentrically loaded steel bridge piers. Recently, several cyclic and pseudodynamic tests have been carried out at Nagoya University on mildly eccentrically loaded steel bridge piers, and the results were compared with test results on centrally loaded specimens by Usami et al[1]. Another important contribution is the numerical study by Ge et al.[2] on the correlation of cyclic behavior between eccentrically loaded and centrally loaded steel bridge piers. Based on this numerical study, it is possible to predict the hysteretic behavior of an eccentrically loaded steel bridge pier from the behavior of its centrally loaded counterpart.

This study makes use of the conclusions of the above mentioned numerical study under static conditions and deals with the inelastic dynamic analysis of eccentrically loaded steel bridge piers modeled as SDOF system. Special problems associated with eccentric loading—modeling of unsymmetrical hysteretic behavior, considering of vertical inertia force are treated first. Effects of eccentricity on seismic responses in ultimate limit state design verification are investigated through a parametric study.

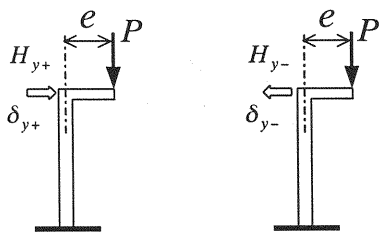

(a) Positive Direction (b) Negative Direction

Fig.2 Definition of yield loads and yield displacements

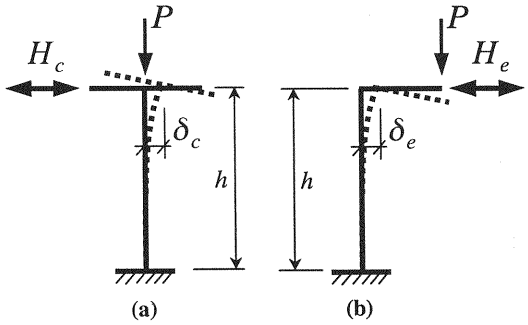

Fig.3 Centrally loaded and eccentrically loaded steel bridge piers

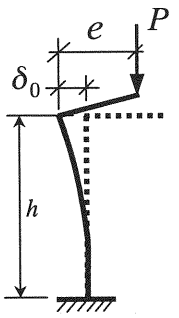

Fig.4 Erection of eccentrically loaded steel bridge piers

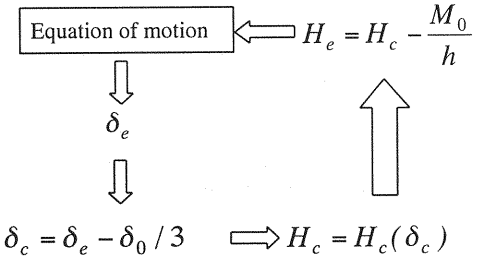

Fig.5 Translation of hysteretic behavior in dynamic analysis

2. MODELING OF HYSTERETIC BEHAVIOR

Compared with centrally loaded steel bridge piers, the in-plane horizontal capacity and hysteretic behavior of eccentrically loaded steel bridge pier becomes unsymmetrical because of the extra bending moment brought about by the vertical load. Defining the direction of eccentric distance as positive, the yield load and yield displacement in the positive direction is going to be smaller than those in the negative direction (**Fig.2**).

Fig.3 shows a pair of centrally loaded and eccentrically loaded steel bridge piers with identical geometrical and material properties and under the action of equal axial force. The yield load for the centrally loaded pier, H_y, can be calculated from the strength equations of steel beam-columns[3] and then the corresponding yield displacement, δ_y, can also be determined. For the eccentrically loaded pier, the yield loads, H_{y+} and H_{y-}, are related to H_y:

$$H_{y+} = H_y - \frac{M_0}{h} \tag{1}$$

$$H_{y-} = H_y + \frac{M_0}{h} \tag{2}$$

wherein $M_0 = P \cdot e$ is the bending moment due to the eccentric load P. It is obvious that H_y is actually the average value of H_{y+} and H_{y-}. The corresponding yield displacements can then be calculated by:

$$\delta_{y+} = \delta_0 + \frac{H_{y+}}{K_e} \tag{3}$$

$$\delta_{y-} = \delta_0 - \frac{H_{y-}}{K_e} \tag{4}$$

in which $\delta_0 = \frac{M_0 \cdot h^2}{2EI}$ is the horizontal displacement due to the bending moment M_0 (EI is cross section modulus), and K_e stands for the elastic horizontal stiffness, and calculated by:

$$K_e = \frac{3EI}{h^3} \tag{5}$$

From Eqs.(1)~(5), the correlation between the yield displacements δ_{y+}, δ_{y-} (measured from the vertical position) and $\delta_y (= H_y / K_e)$ can be obtained as:

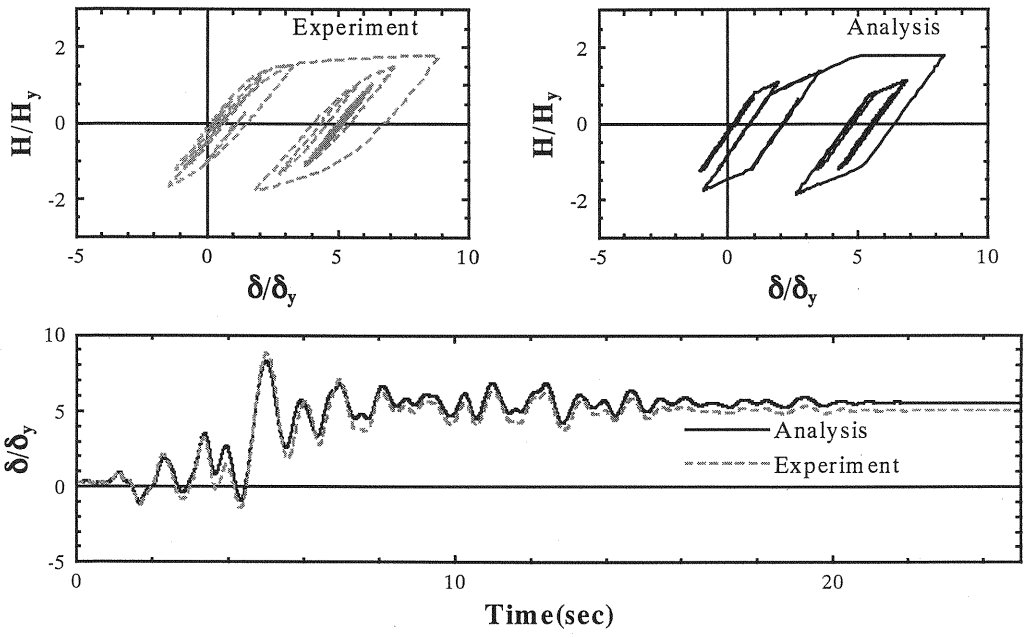

Fig.6 Response of SE35-35H[A] to JR-Takatori accelerogram

$$\delta_{y+} = \delta_y + \frac{\delta_0}{3} \tag{6}$$

$$\delta_{y-} = -\delta_y + \frac{\delta_0}{3} \tag{7}$$

From Eqs.(1)(2)(6)(7), it is clear that within the linear elastic range, there exists a correlation of horizontal hysteretic behavior as follows:

$$H_e(\delta_e) = H_c(\delta_c) - \frac{M_0}{h} \tag{8}$$

$$\delta_c = \delta_e - \frac{\delta_0}{3} \tag{9}$$

Through precise FEM analysis, it was found that the correlation expressed by Eq.(8) is also good for the inelastic range involving even severe local and overall interaction buckling[2]. Thus the prediction of restoring force for centrally loaded steel bridge piers can easily be extended to the prediction for eccentrically loaded steel bridge piers.

In practical construction, an eccentrically loaded bridge pier is usually erected to a leaning position to neutralize the negative influence of eccentric load, so that it comes back to the vertical position when the upper structure is completed (**Fig.4**). In this case, the correlation with the corresponding centrally loaded steel bridge pier shall become[4]:

$$H_e(\delta_e) = H_c(\delta_c) - \frac{M_0}{h} \tag{10}$$

$$\delta_c = \delta_e + \frac{2}{3}\delta_0 \tag{11}$$

It is clear that the only difference between Eq.(8) and Eq.(10) is that δ_0 is measured into δ_e in Eq.(8) while it is excluded from δ_e in Eq.(10). And this difference is equivalent to a shift of reference coordinates, and does not change the essence of the problem.

In the following sections, the damage-based hysteretic model[5), 6), 7)] for thin-walled steel bridge piers is employed to describe H_c, and Eq.(8) (heretofore referred to as the translation equation) is adopted to translate H_c into H_e for seismic response analysis of eccentrically loaded steel bridge piers. Translation of hysteretic behavior in the dynamic analysis procedure is illustrated in **Fig.5**.

3. VERIFICATION OF RESTORING FORCE MODEL

In this section, simulation of two pseudodynamic tests of eccentrically loaded steel bridge piers of stiffened box section[2] is carried out using the damage-based hysteretic model and the translation equation.

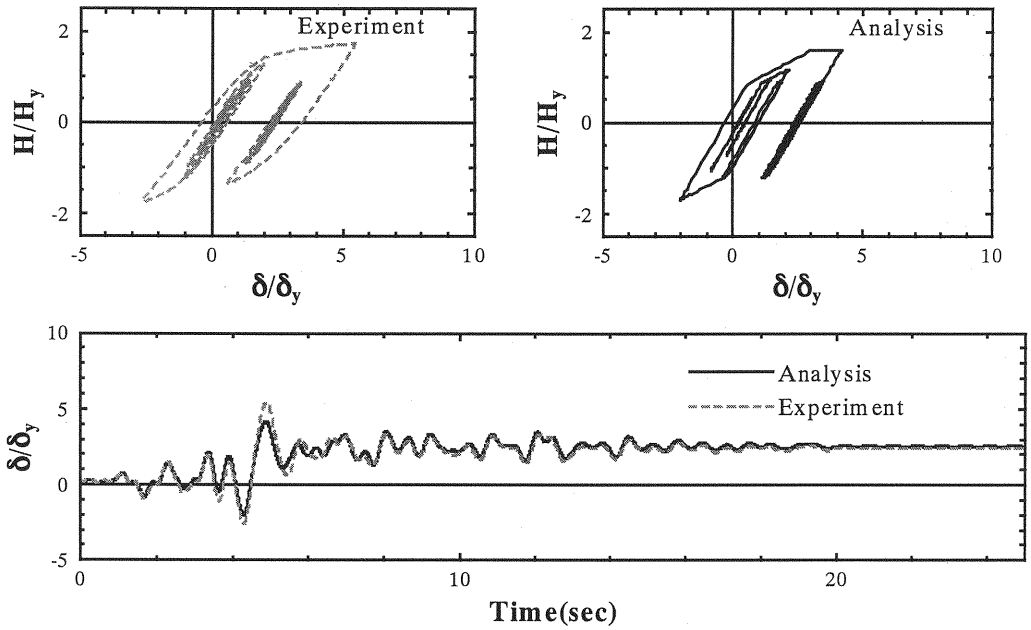

Fig.7 Response of SE35-35H[B] to JR-Takatori accelerogram

Table 1 Parameters of pseudodynamic test specimens

Specimen	SE35-35H[A]	SE35-35H[B]
R_f	0.333	0.335
$\bar{\lambda}$	0.350	0.348
γ / γ^*	3.8	4.0
Aspect ratio	0.5	0.5
e / h	0.0726	0.0726
P / P_y	0.140	0.112
Mass($\times 10^6$kg)	1.79	1.39
T (sec)	0.718	0.638
H_y (kN)	6.59×10^3	6.58×10^3
δ_y (mm)	48.0	48.9
H_{in} / H_y	2.39	1.99
$H_{max,1} / H_y$	2.0	1.75
δ_u / δ_y	33.2	35.2
α	0.3	0.3
β	0.11	0.11
c	1.81	1.80

Note: Mass, H_y, δ_y and the natural period T have been converted to those of the prototype piers (scale factor=8.0).

Input ground motion in both tests is JR-Takatori accelerogram recorded in Hyogoken-Nanbu Earthquake. It is obvious that seismic response of eccentrically loaded steel bridge piers is direction specific due to unsymetric hysteretic characteristics; And in order to reproduce the more severe case of loading, the direction for ground motion input was chosen so that maximum displacement occur on the eccentric side. Tested specimens are two box-section columns proportioned according to the high-ductility criteria (Usami et al. 1996)[8), 9)], and structural parameters of the two specimens are listed in **Table 1**. Due to the limitation of the test machine, eccentric rate e/h (=0.0726) is relatively small compared with existing real bridge piers, and the equation of motion adopted in the tests is:

$$M\ddot{u} + C\dot{u} + H(u) = -M\ddot{x}_g \qquad (12)$$

This equation of motion is the same as that for the centrally loaded specimens, and different from the complete formulation to be introduced in the next section. The vertical inertia force associated with rotation of the overhanging arm in the real steel bridge piers is not taken into consideration. But as will be seen later, it is completely valid for such small e/h . Damping ratio is taken as 0.05 in the tests.

Eq.(12) is also employed in the dynamic

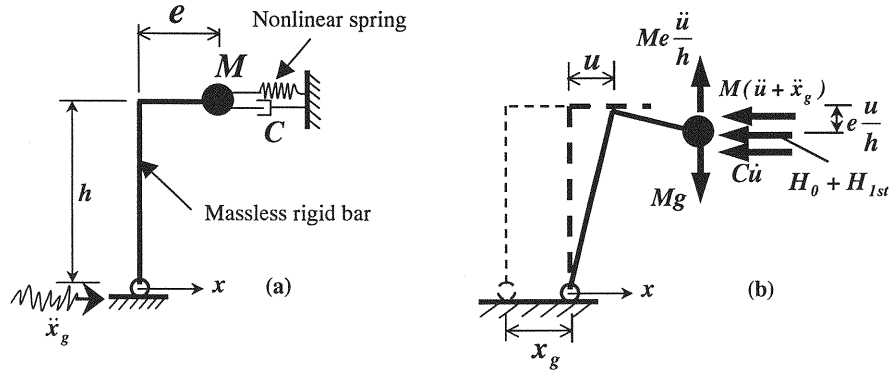

Fig. 8 SDOF modeling of eccentrically loaded steel bridge piers

analysis. Parameters of the damage-based hysteretic model for the test specimens are also listed in **Table 1**. Analysis results are compared with test results in **Fig.6** and **Fig.7**. To facilitate comparison with centrally loaded case, the responses are normalized by H_y and δ_y instead of H_{y+} and δ_{y+}. The good agreement between test results and analysis results indicates that the hysteretic model and the translation equation are valid and adequate for describing hysteretic behavior of eccentrically loaded steel bridge piers.

4. FORMULATION OF EQUATION OF MOTION INCLUDING VERTICAL INERTIA

Fig.8(a) shows the SDOF analytical model for eccentrically loaded steel bridge piers. Since the major contribution to inelastic displacement—local buckling of component plates always occurs near the bottom of the column, the structure is modeled as a massless L-shaped rigid bar attached to the ground by a hinge[10]. The nonlinear spring is responsible for the horizontal restoring force; Ignoring its rotational inertia, the upper structure is modeled by the lumped mass M; And viscous damping is represented by the dash-pot C. From static equilibrium, the eccentric vertical load Mg causes an initial reaction H_0 in the spring:

$$H_0 = \frac{Mg \cdot e}{h} \tag{13}$$

Fig.8(b) illustrates the dynamic equilibrium under a horizontal ground motion $\ddot{x}_g$. Besides the horizontal inertia force $M(\ddot{u}+\ddot{x}_g)$, there is the vertical inertia force due to rotation of the rigid bar: $Me\frac{\ddot{u}}{h}$. And H_{1st} stands for the restoring force of the nonlinear spring. Equilibrium of moment at the hinge yields:

$$\left[M(\ddot{u}+\ddot{x}_g)+C\dot{u}+H_0+H_{1st}\right]\cdot(h-e\frac{u}{h}) + (Me\frac{\ddot{u}}{h}-Mg)\cdot(e+u)=0 \tag{14}$$

Divide both sides of Eq.(14) by h, linearize the equation by omitting higher order terms, notice Eq.(13), and arrange, one arrives at:

$$M(1+\frac{e^2}{h^2})\ddot{u}+C\dot{u}+(H_{1st}-\frac{Mg}{h}\cdot u) - M\frac{e}{h}\frac{\ddot{x}_g}{h}u=-M\ddot{x}_g \tag{15}$$

in which $H_{1st}-\frac{Mg}{h}u$ represents the restoring force in second order theory. Since the restoring force model has taken into account $P-\Delta$ effect, it is clear that

$$H(u)=H_{1st}-\frac{Mg}{h}u \tag{16}$$

Introducing Eq.(16) into Eq.(15), one arrives at the complete equation of motion for eccentrically loaded steel bridge piers under a horizontal ground motion:

$$M\left(1+\frac{e^2}{h^2}\right)\ddot{u}+C\dot{u}+H(u)-M\frac{e}{h}\frac{\ddot{x}_g}{h}u=-M\ddot{x}_g \tag{17}$$

Compared with the equation of motion for centrally loaded steel bridge piers (Eq.(12)), Eq.(17) has on its left-hand side two extra terms: one is $M\frac{e^2}{h^2}\ddot{u}$, which can be regarded as the equivalent vertical inertia; the other is $-M\frac{e}{h}\cdot\frac{\ddot{x}_g}{h}u$, which comes as a direct contribition of eccentricity to the equation of

Table 2 Structural parameters of analyzed eccentrically loaded steel bridge piers

R_f =0.335; $\bar{\lambda}$ =0.348; γ / γ^* =4.0; Aspect ratio=0.5

Bridge Pier	P/P_y	Ground Type	Mass ($\times 10^6$kg)	T (sec)	H_y (kN)	δ_y (mm)
AS-1(e/h=0.1)	0.130	II	1.61	0.657	6.44×10^3	43.6
AS-2(e/h=0.2)	0.105	II	1.30	0.589	6.63×10^3	44.9
AS-3(e/h=0.3)	0.088	II	1.09	0.539	6.76×10^3	45.8
AS-4(e/h=0.4)	0.075	II	0.933	0.499	6.85×10^3	46.4
AS-5(e/h=0.5)	0.066	II	0.818	0.467	6.92×10^3	46.8

motion. Under normal conditions, u/h is rather small, thus the term $-M\frac{e}{h}\cdot\frac{\ddot{x}_g}{h}u$ is expected to have little effect on the overall seismic response. The effect of the equivalent vertical inertia $M\frac{e^2}{h^2}\ddot{u}$ is twofolds: Firstly, it adds to the overall inertia force; Secondly, it will elongate the natural period of the system. Although the differences in both inertia force and natural period are negligible when e/h is small (e.g., when e/h =0.1, the inertia force is amplified by only 1%, and the difference in natural period is less than 0.5%), they may become considerable when e/h becomes relatively large (In case e/h =0.5, the difference in inertia force is 25% and the natural period is elongated by nearly 12%). Thus including the vertical inertia may have quite a influence on the computed seismic response.

The above estimations about the influence of these two extra terms of Eq.(17) are verified by the following numerical experiment: Three formulations of equation of motion are employed to predict seismic response to JR-Takatori accelerogram; Formulation A corresponds to Eq.(17) — the complete equation of motion; Formulation B stands for the following reference equation:

$$M(1+\frac{e^2}{h^2})\ddot{u}+C\dot{u}+H(u)=-M\ddot{x}_g \qquad (18)$$

which just excludes the term $-M\frac{e}{h}\cdot\frac{\ddot{x}_g}{h}u$ from Eq.(17). And Formulation C refers to Eq.(12), which is the same equation of motion for centrally loaded steel bridge piers. The numerical experiment is carried out on five box-section specimens (parameters listed in **Table 2**) designed with different eccentricity rate e/h =0.1, 0.2, 0.3, 0.4, 0.5 respectively. It turns out that the difference between the predicted responses by Eq.(17) and Eq.(18) is almost undetectable under all e/h values. However, the difference between results from Eq.(17) and those from Eq.(12) varies case by case as shown in **Fig.9** : For the case e/h =0.1, predicted responses by the two equations almost coincide with each other; from e/h =0.2 and on, the difference becomes noticeable; There is conspicuous difference in maximum and residual displacements in the case of e/h =0.4; And difference in natural period is reflected most vividly in the case of e/h =0.5 . It can also be seen from this numerical example that although vertical inertia will add to the overall inertia force in the equation of motion, including vertical inertia does not necessarily result in larger response: In **Fig.9**, the predicted response based on Eq.(17) is larger than that based on Eq.(12) in the case of e/h =0.2, while this comparison is reversed in the case of e/h =0.4 . This phenomenon indicates that variation in natural period resulted from the vertical inertia also has a considerable weight in determining the computed response.

Conlusion from this numerical experiment is that the complete equation of motion for eccentrically loaded steel bridge piers—Eq.(17) can safely be simplified to Eq.(18), but further simplification to Eq.(12) is only justified under small e/h (preferably $\leqq$ 0.1). Looking back at the pseudodynamic tests of the previous section, it can be seen that Eq.(12) can work just as well under the test conditions, since e/h is only 0.0726.

5. PARAMETRIC STUDY

Effect of eccentricity on the seismic response is of major concern in the ultimate limit state design of eccentrically loaded steel bridge piers. Based on the complete equation of motion, a parametric study is carried out with e/h =0.0, 0.1, 0.2, 0.3, 0.4, 0.5 (e/h =0.0 means the centrally loaded steel bridge piers set up for comparison) under Level 2 design earthquake accelerograms. Besides e/h, the natural period is also taken as a parameter of concern and the results are presented in the form of maximum displacement and residual displacement spectra.

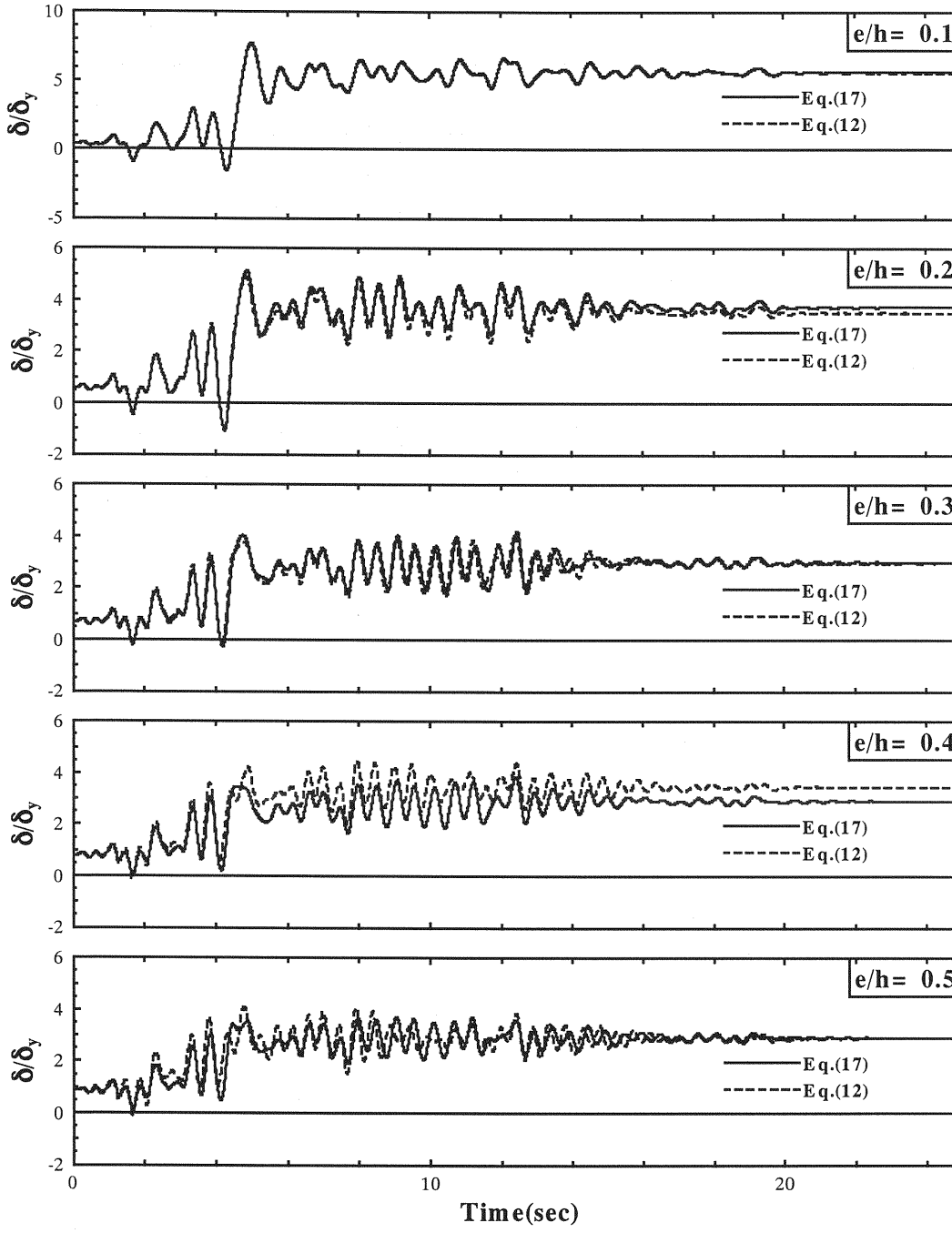

Fig.9 Effect of vertical inertia on calculated responses

Table 3 Axial load ratio P/P_y and natural period ***T (second)*** of analyzed bridge piers

Specimen No.	e / h	$\bar{\lambda}$	P/P_y			T (second)		
			G.T. I	G.T. II	G.T. III	G.T. I	G.T. II	G.T. III
S1	0.0	0.20	0.284	0.243	0.212	0.482	0.445	0.416
S2		0.25	0.243	0.206	0.178	0.622	0.573	0.533
S3		0.30	0.212	0.178	0.154	0.765	0.701	0.651
S4		0.35	0.188	0.158	0.135	0.908	0.830	0.769
S5		0.40	0.169	0.141	0.121	1.05	0.960	0.888
S6		0.45	0.164	0.128	0.109	1.24	1.09	1.01
S7		0.50	0.164	0.117	0.099	1.45	1.22	1.13
S8	0.1	0.20	0.212	0.188	0.169	0.416	0.392	0.372
S9		0.25	0.178	0.158	0.141	0.533	0.501	0.474
S10		0.26		0.153			0.523	
S11		0.27		0.148			0.545	
S12		0.30	0.154	0.135	0.121	0.651	0.611	0.577
S13		0.32		0.128			0.654	
S14		0.33		0.125			0.676	
S15		0.34		0.122			0.698	
S16		0.35	0.135	0.119	0.106	0.769	0.720	0.680
S17		0.37		0.113			0.764	
S18		0.40	0.121	0.106	0.094	0.888	0.830	0.783
S19		0.45	0.109	0.095	0.084	1.01	0.940	0.886
S20		0.50	0.100	0.087	0.077	1.13	1.05	0.990
S21	0.2	0.20	0.169	0.154	0.141	0.372	0.354	0.339
S22		0.25	0.141	0.128	0.117	0.474	0.451	0.431
S23		0.30	0.121)	0.109	0.099	0.577	0.548	0.523
S24		0.35	0.106	0.095	0.087	0.680	0.645	0.615
S25		0.40	0.094	0.084	0.077	0.783	0.742	0.708
S26		0.45	0.084	0.076	0.069	0.886	0.840	0.800
S27		0.50	0.076	0.069	0.062	0.989	0.937	0.892
S28	0.3	0.20	0.141	0.130	0.122	0.339	0.326	0.316
S29		0.25	0.117	0.107	0.099	0.431	0.414	0.398
S30		0.30	0.099	0.091	0.084	0.523	0.501	0.482
S31		0.35	0.086	0.079	0.073	0.615	0.589	0.566
S32		0.40	0.077	0.070	0.065	0.708	0.677	0.651
S33		0.45	0.069	0.063	0.058	0.800	0.765	0.735
S34		0.50	0.062	0.057	0.053	0.892	0.854	0.819
S35	0.4	0.20	0.121	0.113	0.107	0.314	0.303	0.296
S36		0.25	0.099	0.093	0.087	0.398	0.384	0.371
S37		0.30	0.084	0.078	0.073	0.482	0.465	0.449
S38		0.35	0.073	0.068	0.064	0.566	0.546	0.528
S39		0.40	0.065	0.060	0.056	0.651	0.627	0.606
S40		0.45	0.058	0.054	0.050	0.735	0.708	0.684
S41		0.50	0.053	0.049	0.046	0.819	0.789	0.762

Table 3 (Continue) Axial load ratio P/P_y and natural period T *(second)* of analyzed bridge piers

Specimen No.	e/h	$\bar{\lambda}$	P/P_y			T *(second)*		
			G.T. I	G.T. II	G.T. III	G.T. I	G.T. II	G.T. III
S42	0.5	0.20	0.106	0.099	0.096	0.294	0.285	0.280
S43		0.25	0.087	0.081	0.077	0.371	0.360	0.350
S44		0.30	0.073	0.069	0.065	0.449	0.435	0.423
S45		0.35	0.064	0.060	0.056	0.528	0.511	0.496
S46		0.40	0.056	0.053	0.050	0.606	0.586	0.569
S47		0.45	0.050	0.047	0.044	0.684	0.662	0.642
S48		0.50	0.046	0.043	0.040	0.762	0.737	0.715

Analyzed specimens are of stiffened box-section proportioned by elastic seismic design according to current Design Specifications of Highway Bridges of Japan Road Association[10]. Measuring up to the high-ductility criteria[7][8] for stiffened box-section steel bridge piers is also considered, and the following uniform structural parameters are chosen: width-thickness ratio of the flange plates R_f =0.35; stiffness ratio of the longitudinal stiffeners $\gamma/\gamma^* = 3$; and the aspect ratio of flange plate between diaphragms =0.5 . **Table 3** gives the axial load ratio and natural period of all analyzed specimens, and the natural period is calculated according to the following equation:

$$T = 2\pi\sqrt{\frac{M}{K_e}} \tag{19}$$

Eq.(19) does not account for the difference brought about by vertical inertia, but offers a standard measurement regardless of e/h value. Damping coefficient C is calculated by:

$$C = 2\xi\sqrt{K_e M} \tag{20}$$

in which damping ratio ξ is taken as 0.05.

The response spectra under Type I and Type II accelerograms are given in **Fig.10** and **Fig.11** respectively. They are made from averaging the maximum responses to three accelerograms contained in each group.

From the maximum displacement spectra under both Type I and Type II accelerograms, it is clear that the most dangerously strained group is neither the centrally loaded nor the group with e/h =0.5; Instead, it is the mildly eccentrically loaded specimens with e/h around 0.1~0.2 that have the highest maximum response. This can be explained by the fact that although eccentricity by itself tends to exacerbate seismic damage, the vertical load from the upper structure becomes smaller for larger e/h in the elastic seismic design, which has the effect of mitigate seismic response; And the combined effect of large vertical load (system mass) and eccentricity is responsible for the large response of mildly eccentrically loaded specimens.

On the other hand, the trend in residual displacement is somewhat different: under both Type I and Type II accelerograms of all kinds of ground conditions: the centrally loaded specimens always have the lowest level of residual displacement. It seems that eccentricity will cause inelastic displacement to gravitate toward the eccentric side, and makes it harder to return to neutral. The same trend on residual displacement has also been reported in Ref. 1) from comparison of pseudodynamic test results on centrally loaded and eccentrically loaded steel bridge piers.

6. CONCLUSIONS

In previous sections, seismic response analysis of eccentrically loaded steel bridge piers is tackled by a simple SDOF dynamic formulation which takes into account the vertical inertia associated with horizontal ground motion. Effects of eccentricity on the predicted responses under Level 2 design accelerograms are investigated based on the proposed dynamic analysis approach. Major findings and conclusions are summarized as follows:

(1) Through the translation equation, modeling of hysteretic behavior for eccentrically loaded steel bridge piers becomes equivalent to modeling for the centrally loaded steel bridge piers. And any appropriate SDOF hysteretic model for centrally loaded steel bridge piers can also be made use of in seismic response analysis of eccentrically loaded steel bridge piers.

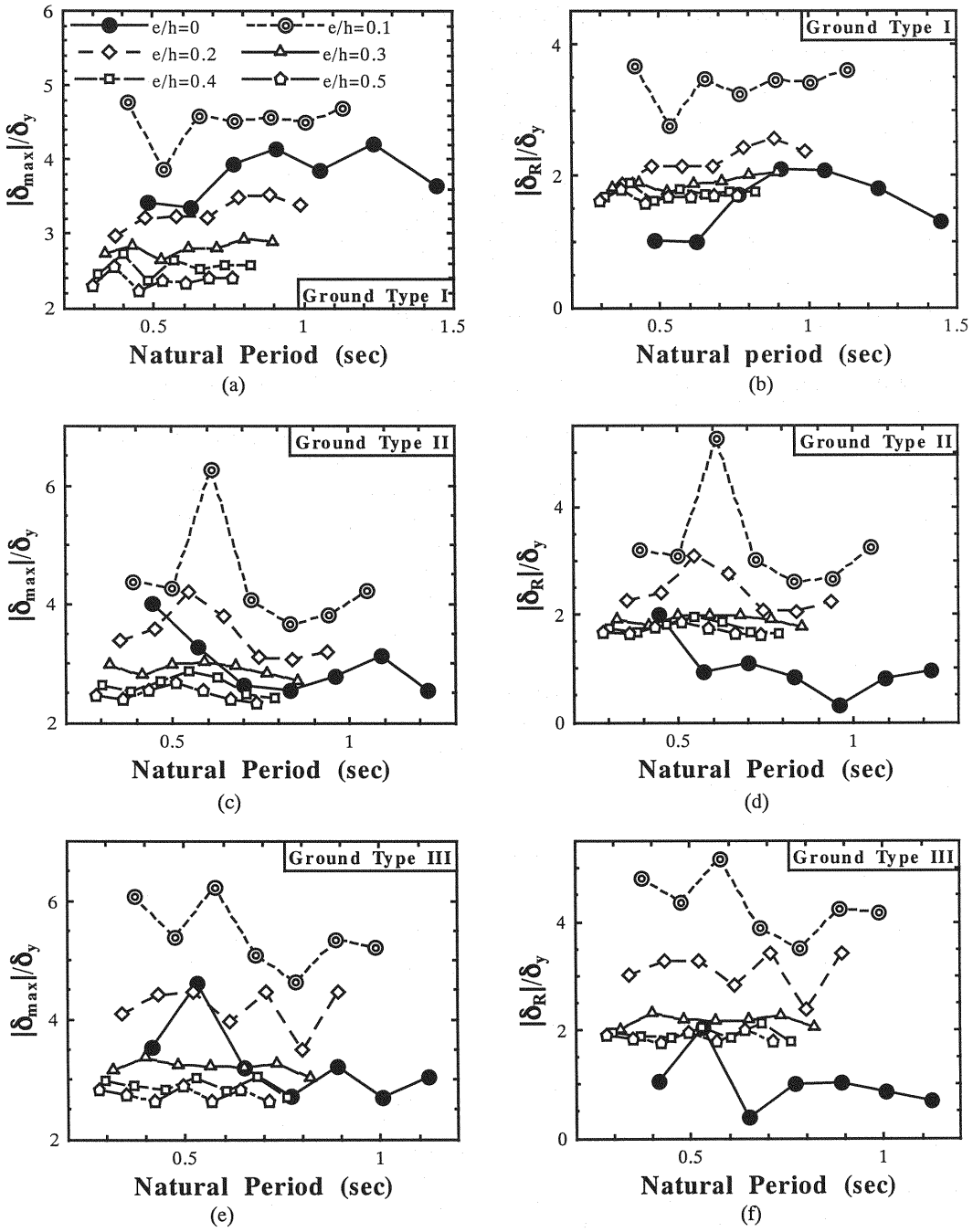

Fig.10 Response spectra under Level 2 Type I accelerograms

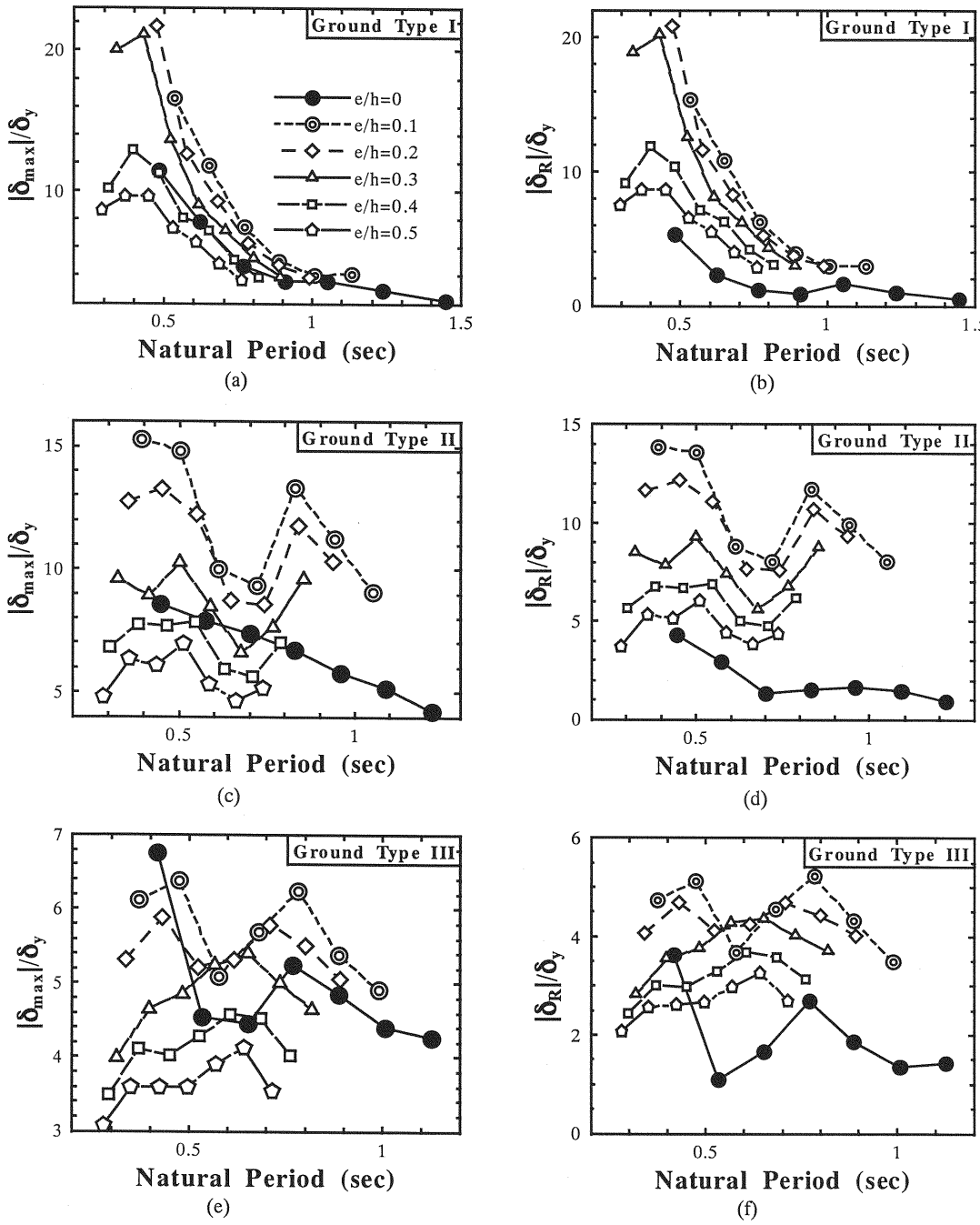

Fig.11 Response spectra under Level 2 Type II accelerograms

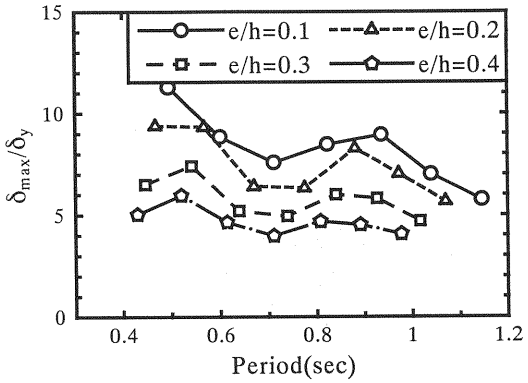

Fig.A1 Response spectra of specimens designed under constant $P_{central}$

(2) When e/h is relatively small, including vertical inertia in the analysis almost makes no difference on the predicted response. However, in case of relatively large e/h, it is necessary to consider vertical inertia and use Eq.(18) for seismic response analysis of eccentrically loaded steel bridge piers.

(3) Including vertical inertia will amplify the overall inertia force and elongate the natural period of the system. Effect of vertical inertia on the amplitude of predicted response varies from case to case; It does not necessarily lead to larger computed response.

(4) Eccentrically loaded steel bridge piers with e/h around 0.1~0.2 tend to have the highest level of maximum displacement response among all eccentrically loaded piers designed under the same conditions based on the seismic coefficient method. However, with higher value of e/h, the maximum displacement response tends to become lower due to the fact that load from the upper structure goes lower in the elastic seismic design by the seismic coefficient method. The maximum displacement response of centrally loaded steel bridge piers usually comes between the highest level corresponding to those with e/h around 0.1~0.2 and the lowest level corresponding to those with e/h of 0.4 or 0.5 .

(5) Designed under the same conditions, eccentrically loaded steel bridge piers will generally have higher level of residual displacement than centrally loaded piers, which may be a matter of concern in practical design.

APPENDIX

The parametric study of this paper is carried out with e/h as the major parameter and all the specimens have a uniform cross section (stiffened box section made of SM490 constructional steel with width-thickness ratio of the flange plates R_f =0.35; stiffness ratio of the longitudinal stiffeners $\gamma/\gamma^* = 3$, the aspect ratio of flange plate between diaphragms =0.5, radius of gyration r =764.9mm, and component plate thickness t =23mm). Then, the load from the upper structure is determined according to seismic coefficient method. In this part, the parametric study is carried out further following a different course in specimen design: Firstly, the load from the upper structure is calculated assuming centrally loaded condition for all the specimens in the parametric study. Then, keeping this vertical load, the thickness of

Table A1 Axial load ratio P/P_y and natural period T *(second)* of specimens designed with constant $P_{central}$

Specimen No.	e/h	$\bar{\lambda}$	G.T.II	
			P/P_y	T *(second)*
AS1	0.1	0.20	0.183	0.495
AS2		0.25	0.152	0.600
AS3		0.30	0.131	0.711
AS4		0.35	0.114	0.823
AS5		0.40	0.100	0.936
AS6		0.45	0.086	1.040
AS7		0.50	0.075	1.146
AS8	0.2	0.20	0.146	0.468
AS9		0.25	0.120	0.567
AS10		0.30	0.102	0.670
AS11		0.35	0.089	0.775
AS12		0.40	0.078	0.881
AS13		0.45	0.065	0.972
AS14		0.50	0.056	1.070
AS15	0.3	0.20	0.121	0.447
AS16		0.25	0.100	0.542
AS17		0.30	0.084	0.639
AS18		0.35	0.073	0.739
AS19		0.40	0.064	0.840
AS20		0.45	0.052	0.926
AS21		0.50	0.045	1.017
AS22	0.4	0.20	0.104	0.431
AS23		0.25	0.085	0.521
AS24		0.30	0.072	0.614
AS25		0.35	0.062	0.711
AS26		0.40	0.054	0.808
AS27		0.45	0.044	0.892
AS28		0.50	0.037	0.977

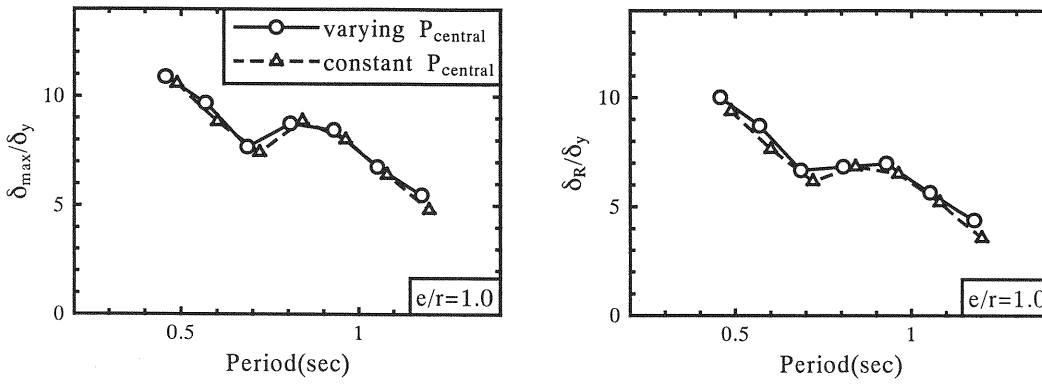

Fig.A2 Comparison of response spectra with the major parameter of e/r

Table A2 Axial load ratio P/P_y and natural period T *(second)* of specimens designed with parameter e/r

Specimen No.	e/r	$\bar{\lambda}$	G.T.II	
			P/P_y	T *(second)*
AS-V1	1.0	0.20	0.180	0.457
AS-V2		0.25	0.159	0.569
AS-V3		0.30	0.143	0.685
AS-V4		0.35	0.129	0.805
AS-V5		0.40	0.118	0.928
AS-V6		0.45	0.108	1.053
AS-V7		0.50	0.100	1.108
AS-P1	1.0	0.20	0.173	0.489
AS-P2		0.25	0.152	0.600
AS-P3		0.30	0.137	0.719
AS-P4		0.35	0.124	0.840
AS-P5		0.40	0.112	0.962
AS-P6		0.45	0.101	1.081
AS-P7		0.50	0.091	1.201

Note: AS-V1 AS-V7 are designed under varying $P_{central}$; AS-P1 AS-P7 are designed under constant $P_{central}$.

component plate is redesigned taking into account eccentricity (Heretofore, this course of specimen design is inappropriately referred to as constant $P_{central}$ case for simplicity while the former course of specimen design is referred to as varying $P_{central}$ case). **Fig.A1** shows the maximum displacement spectra under Level 2 Type II Ground Type II accelerograms, and **Table A1** lists the axial load ratio and natural period of the analyzed specimens (design conditions common to all the specimens are: stiffened box section made of SM490A constructional steel; width-thickness ratio of the flange plates R_f =0.35; stiffness ratio of the longitudinal stiffeners $\gamma / \gamma^* = 3$; the aspect ratio of flange plate between diaphragms =0.5). It can be seen that although the specific responses are different from those reflected in **Fig.11(c)** under each e/h value (the responses become lower compared with the constant $P_{central}$ case), the general trend in responses with varying e/h remains the same. And the same can be said of residual displacement spectra.

The above discussion points out that the response spectra with the same e/h will be different if the design of specimen takes different courses. If the ratio of eccentric distance to the radius of gyration e/r is taken as the major parameter instead of e/h, the resulted response spectra will become much closer to each other under the above two different courses of specimen design. **Fig.A2** compares the spectra with e/r =1.0. **Table A2** gives the axial load ratio and natural period of the analyzed specimens (design conditions common to all the specimens are kept as the same as in the discussion above). However, when e/r =2.0, it is observed that although the shapes of the response spectra are very similar, the difference in responses still can not be neglected under different courses of specimen design. Accordingly, a universal parameter to define eccentricity is still to be found if the most general response spectra are to be plotted for eccentrically loaded steel bridge piers.

REFERENCES

1) Usami, T., Honma, D. and Yoshizaki, K.: Pseudodynamic tests of eccentrically loaded steel bridge piers, *J. Struct. Mech. and Earth. Engrg*, JSCE, No.626/I-48, pp.197-206, 1999 (In Japanese).
2) Ge, H. B., Gao, S. B. and Usami, T.: Numerical study on

cyclic elastoplastic behavior of eccentrically loaded steel bridge piers, to appear in *J. Struct. Mech. and Earth. Engrg*, JSCE, 2000(In Japanese).
3) Usami, T., Mizutani, S., Aoki, T. and Itoh, Y.: Steel and concrete-filled steel compression members under cyclic loading, Stability and Ductility of Steel Structures Under Cyclic Loading, Edited by Fukumoto, Y. and Lee, G. C., pp.123-128, CRC Press, Boca Raton, Fl, 1992.
4) Gao, S. B., Usami, T. and Ge, H. B.: Numerical Study on Seismic Performance Evaluation of Steel Structures, NUCE Research Report No. 9801, Dept. of Civil Engineering, Nagoya University, 1998.
5) Kumar, S. and Usami, T.: An evolutionary-degrading hysteretic model for thin-walled steel structures, *Engineering Structures*, Vol. 18, No.7, pp.504-514, 1996.
6) Kindaichi, T., Usami, T. and Kumar, S.: A hysteresis model based on damage index for steel bridge piers, *Journal of Structural Engineering, JSCE*, Vol. 44A, pp.667-678, March, 1998 (In Japanese).
7) Liu, Q. Y., Kasai, A. and Usami, T.: Inelastic response spectra for seismic design verification of pipe and stiffened box steel bridge piers, submitted to *Journal of Structural Engineering, JSCE*, 2000.
8) Usami, T., Watanabe, K., Kindaichi, T., Okamoto, S. and Ikeda, S.: Experimental study on seismic performance of high-ductility steel bridge piers, *J. Struct. Mech. and Earth. Engrg*, JSCE, No.591/I-43, pp.207-218, April, 1998 (In Japanese).
9) Usami, T.: High-ductility steel bridge piers, *Bridge and Foundation*, Vol.31, No.6, pp.30-36, June, 1997.
10) M. Abe and Y. Fujino, Effect of rotational inertia and eccentric loading on seismic response of T-shaped bridge piers, Proceedings of the 24th JSCE Earthquake Engineering Symposium, Vol.2, pp.1005-1008, July, 1997.
11) Design Specifications of Highway Bridges (Part V. Seismic Design), Japan Road Association, December 1996 (In Japanese).

(Received April 23, 1999)